BMC Medical Imaging

RESEARCH Open Access

Identification of triple-negative breast cancer and androgen receptor expression based on histogram and texture analysis of dynamic contrast-enhanced MRI

Wen-juan Xu[1], Bing-jie Zheng[1], Jun Lu[1], Si-yun Liu[2] and Hai-liang Li[1*]

Abstract

Background Triple-negative breast cancer (TNBC) is highly malignant and has a poor prognosis due to the lack of effective therapeutic targets. Androgen receptor (AR) has been investigated as a possible therapeutic target. This study quantitatively assessed intratumor heterogeneity by histogram analysis of pharmacokinetic parameters and texture analysis on dynamic contrast-enhanced magnetic resonance imaging (DCE-MRI) to discriminate TNBC from non-triple-negative breast cancer (non-TNBC) and to identify AR expression in TNBC.

Methods This retrospective study included 99 patients with histopathologically proven breast cancer (TNBC: 36, non-TNBC: 63) who underwent breast DCE-MRI before surgery. The pharmacokinetic parameters of DCE-MRI (K^{trans}, K_{ep} and V_e) and their corresponding texture parameters were calculated. The independent t-test, or Mann-Whitney U-test was used to compare quantitative parameters between TNBC and non-TNBC groups, and AR-positive (AR+) and AR-negative (AR-) TNBC groups. The parameters with significant difference between two groups were further involved in logistic regression analysis to build a prediction model for TNBC. The ROC analysis was conducted on each independent parameter and the TNBC predicting model for evaluating the discrimination performance. The area under the ROC curve (AUC), sensitivity and specificity were derived.

Results The binary logistic regression analysis revealed that K_{ep_Range} ($p = 0.032$) and $V_{e\_SumVariance}$ ($p = 0.005$) were significantly higher in TNBC than in non-TNBC. The AUC of the combined model for identifying TNBC was 0.735 ($p < 0.001$) with a cut-off value of 0.268, and its sensitivity and specificity were 88.89% and 52.38%, respectively. The value of $K_{ep\_Compactness2}$ ($p = 0.049$), $K_{ep\_SphericalDisproportion}$ ($p = 0.049$), and $V_{e\_GlcmEntropy}$ ($p = 0.008$) were higher in AR + TNBC group than in AR-TNBC group.

Conclusion Histogram and texture analysis of breast lesions on DCE-MRI showed potential to identify TNBC, and the specific features can be possible predictors of AR expression, enhancing the ability to individualize the treatment of patients with TNBC.

*Correspondence:
Hai-liang Li
hailiangligr@163.com

Full list of author information is available at the end of the article

Keywords Breast cancer, Triple-negative breast cancer, Dynamic contrast-enhanced MRI, Texture analysis, Androgen receptor

Introduction

Breast cancer is the most prevalent cancer in the world and has a high mortality rate [1]. According to the St Gallen International Expert Panel, invasive breast cancer is divided into five distinct subtypes based on microarray profiling: luminal A, luminal B, luminal-human epidermal growth factor receptor 2 (HER2), HER2-enriched, and triple negative (TN) [2]. Triple-negative breast cancer (TNBC) is defined by immunohistochemistry (IHC) as the lack of expression of estrogen receptor (ER), progesterone receptor (PR), and HER2 [3]. Compared with other subtypes of breast cancer, TNBC has an increased possibility of distant recurrence and death [4]. Currently, the treatment of breast cancer is largely guided by ER, PR and HER2 status: ER+/PR+patients require effective endocrine therapy; HER2+patients require anti-HER2 targeted therapy; however, due to the lack of effective therapeutic targets for TNBC, there is no specific targeted therapy available. As a result, it has limited treatment options and is usually treated with cytotoxic therapy with poor clinical efficacy [5]. Therefore, it is important to distinguish TNBC from non-TNBC and to find new therapeutic targets for TNBC.

By adopting unsupervised clustering analyses with genomic data on cases of TNBC, six molecular subtypes of TNBC have been identified by Lehmann et al. [6], which have shown that TNBC is remarkably heterogeneous at the transcriptional level. Among them, the luminal androgen receptor (LAR) subtype characterized by androgen receptor (AR) expression is a subtype that deserves special attention.

AR has been reported as a prognostic biomarker that provides additional information and may be a viable therapeutic target for TNBC [7]. AR is highly expressed in 10–50% of TNBC [7]. According to some recent studies, AR has been shown to be a biomarker associated with poor prognosis in TNBC in terms of disease-free survival and overall survival [8]. The LAR subtype had a relatively lower proliferation rate, lower recurrence-free survival and similar distant metastasis-free survival compared with other subtypes [9]. Retrospective evaluation of patients undergoing neoadjuvant system therapy showed that LAR subtype is associated with lower pathologically complete response rates [10]. Furthermore, AR is under clinical investigation as a therapeutic target for TNBC [11, 12]. Therefore, identifying TNBC and judging the expression of AR in TNBC are of great significance in selecting treatment options and predicting treatment efficacy. If the presence of TNBC and the expression of AR in TNBC can be determined prior to surgery, it is possible to determine whether the patient is suitable for neoadjuvant chemotherapy and which regimen should be used. The identification of molecular subtypes and AR expression are mainly dependent on biopsy. However, due to the heterogeneity of the tumor, in up to 20% of patients, there is a difference in the receptor status between biopsy samples and postoperative samples [13]. Non-invasive prediction of molecular subtypes and AR expression based on MRI is a promising method to reflect the biology of the entire tumor and contribute to more accurate diagnosis and treatment. Therefore, numerous studies have attempted to use diffusion weighted imaging (DWI) [14, 15], DCE-MRI [16, 17], and other MRI sequences to differentiate molecular subtypes of breast cancer [18, 19]. However, there are few studies using MRI to distinguish whether AR is expressed in TNBC [20].

Among these sequences, DCE-MRI is considered the most sensitive method for detecting breast cancer. Some researchers looking at the image features on DCE-MRI found that the rim and persistent enhancement pattern of tumors were useful features for detecting TNBC [19]. Since the image characteristics of tumors are susceptible to the subjective influence of radiologists, some studies have attempted to identify TNBC with semi-quantitative parameters of DCE-MRI [21]. With the advancement of quantitative DCE-MRI based on pharmacokinetic models, there is an increasing interest in novel DCE-MRI-based biomarkers for identifying different molecular subtypes of breast cancer. Most of the relevant studies are histogram analysis that based on pharmacokinetic parameters [22]. The histogram is related to the gray-scale frequency distribution of pixel intensities within the region of interest, and it provides a simple, visual representation of the statistical information contained in the image [23]. Histogram analysis based on pharmacokinetic parameters can reflect the blood perfusion of the tumor [24]. Researches in recent years have shown that texture analysis can reveal more information about heterogeneous tumor components [25]. Texture features quantify the gray-level changes within the image and contain deep information about the structural and organizational arrangement of the object and its connection with the surrounding environment.

Histogram and texture analysis of DCE-MRI can reveal more information about the heterogeneous tumor components [26]. We attempted to use histogram and texture features derived from multiple DCE-MRI parametric maps to noninvasively and preoperatively discriminate between TNBC and non-TNBC and identity whether AR is highly expressed in TNBC.

Materials and methods

Patient selection

As a retrospective study, we searched for 543 breast cancer patients who underwent breast DCE-MRI and subsequent treatment at our institution from June 2020 to August 2021. Inclusion criteria: (I) Patients with histologically confirmed invasive breast cancer and IHC findings including expression of AR, ER, PR, HER2 and Ki-67. (II) Patients underwent DCE-MRI within two weeks before surgery. (III) Patients with complete DCE-MRI data. (IV) Patients whose image quality and shooting conditions met the diagnostic criteria. Exclusion criteria: (I) Patients who received radiotherapy, neoadjuvant chemotherapy, or surgery before imaging. (II) Patients with incomplete DCE-MRI data or poor image quality. (III) Patients with other malignant tumors. (IV) Patients with incomplete pathological and immunohistochemical information. Finally, 99 female patients (mean age: 52.85±10.15 years, range: 30–78 years) with 99 breast cancers (TNBC [n=36], non-TNBC [n=63]) were enrolled in this study. The study was conducted in accordance with the Declaration of Helsinki. The Life Science Ethics Committee of Zhengzhou University approved this retrospective analysis and waived the need for informed consent.

DCE-MRI image acquisition

All examinations were performed on a 3.0 T Skyra device (Siemens Healthcare, Erlangen, Germany) using a 16-channel bilateral breast coil (Siemens Healthcare, Erlangen, Germany) with the patient positioned in the center of the magnet in the prone position. After routine fat-suppressed T2-weighted imaging, 3D gradient echo sequences with volumetric interpolated breath-hold examination at different flip angles (3°and 15°) were acquired for T1 mapping with the following parameters: repetition time (TR), 5.01 ms; echo time (TE), 2.26 ms; field of view (FOV), 340×340 mm^2; slice thickness, 2.0 mm; matrix, 224×166; and total acquisition time (TA), 2 min 35 s. Next, DCE-MRI was performed using time-resolved angiography with interleaved stochastic trajectories sequence and the following parameters: TR, 4.18 ms; TE, 1.31 ms; FOV, 640×560 mm^2; slice thickness, 2.0 mm; no gap; matrix, 320×249; flip angle, 12°; temporal resolution, 7.84 s/phase; and TA, 5 min 33 s. At the beginning of the fourth DCE-MRI frame acquisition, Gd-DTPA-BMA (0.2 mmol/kg; Omni-Scan, GE Healthcare, Ireland) was injected intravenously using a power injector at a flow rate of 2.5 mL/s, followed by a 20-mL saline-flush. T1 mapping and DCE-MRI were performed in the axial plane, and bilateral breast images were acquired.

Postprocessing of MRI Data

Raw DCE-MRI scan data were analyzed with a dedicated post-processing software (Omni-Kinetics; GE Healthcare, Milwaukee, WI). Two radiologists (BZ and WX) with 9 and 2 years of experience in the interpretation of breast MRI, who were blinded to the patients' histopathological results, participated in this study. The enhancement kinetics were analyzed on the basis of the Extended Tofts Linear mode, and then the post-processing software automatically generated voxel-wise perfusion maps. Patient-specific artery input functions (AIFs) were measured, and tumor region of interest (ROI) was manually defined by radiologists on each axis of the lesion DCE-MRI sequence. Each layer of ROI included as much tumor tissue as possible, including any cystic, necrotic, or hemorrhagic components, for better assessment of tumor heterogeneity. To reduce the partial volume effect, the ROI was slightly smaller than the actual tumor size. Then, the workstation merged all ROIs into a volume of interest (VOI). The workflow was shown in Fig. 1. Finally, three pharmacokinetic parameters were extracted by the software, and the histograms and texture features corresponding to these parameters were also extracted. These parameters are K^{trans} (the transfer constant of the contrast agent from the plasma compartment into the extravascular extracellular space [EES], min^{-1}), K_{ep} (the rate constant of the escape of the contrast agent from the EES into the plasma compartment, min^{-1}), and V_e (the EES per unit volume of tissue, mL/100 mL of tissue, %).

To evaluate the interobserver agreement to verify the reliability and stability of these parameters, radiologist WX performed tumor measurements on all 99 patients and radiologist BZ performed tumor measurements on 50 patients randomly selected from the entire cohort. The parameters with interclass correlation coefficient (ICC) values greater than 0.75 for further analysis.

Histopathologic assessment

The histopathological and immunohistochemical information was confirmed by surgical specimen. IHC analysis was used to determine the expression of ER, PR, AR, HER-2 and Ki-67. The expression of ER and PR was estimated by staining the cell nuclei; when the percentage of positive cells was higher than 1%, it was considered positive. HER2 status was determined by IHC or fluorescence in situ hybridization (FISH), an IHC score 3+was defined as positive; when the IHC score was 2+, FISH was performed to assess gene amplification, and HER2 was considered positive if the ratio≥2.0; while an IHC score 0 or 1+was defined as negative. High expression of Ki-67 was defined as the presence of ≥14% positively stained nuclei. TNBC is defined as ER-negative, PR-negative and HER2-negative. The AR status was defined as positive if≥1% of tumor cells showed positive staining.

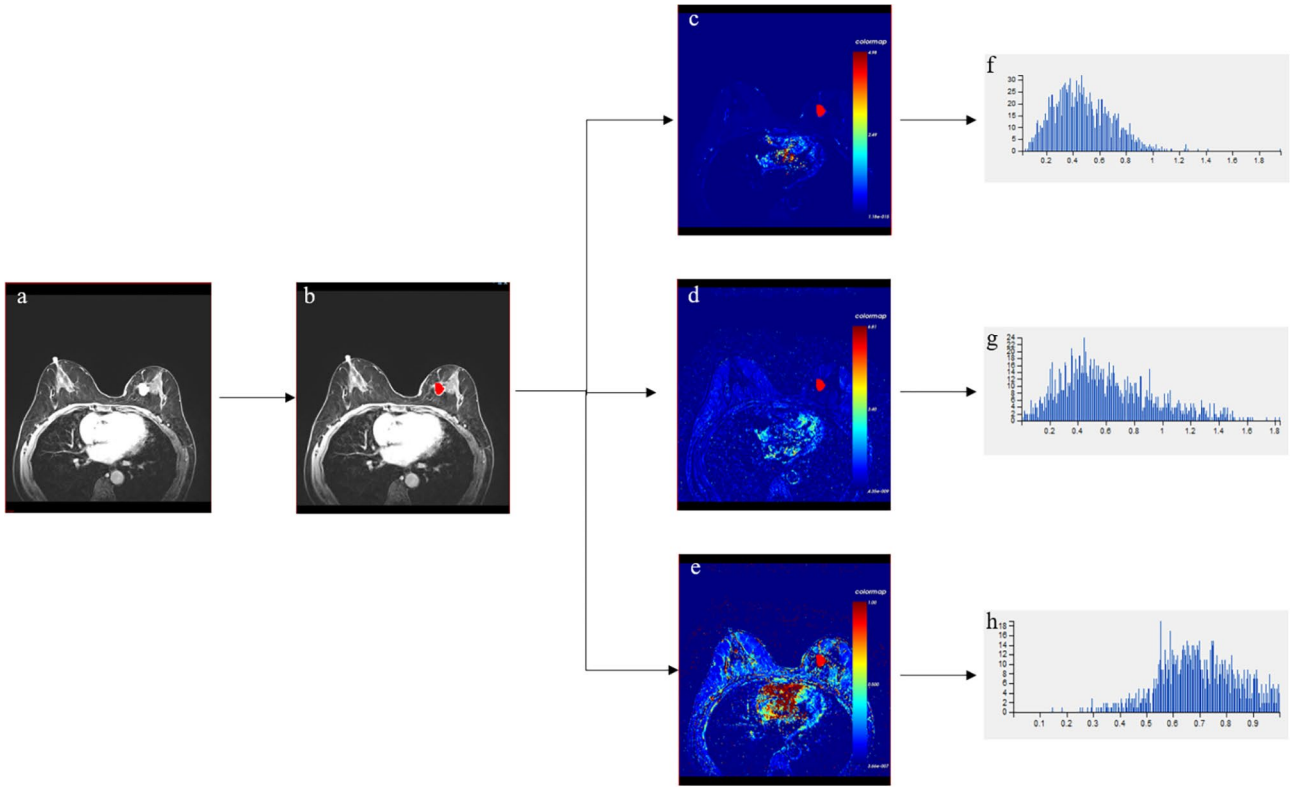

Fig. 1 The workflow diagram shows the voxel analysis process for a tumor. (**a**) Post-contrast images. (**b**) ROI selection of tumor. (**c**) K^{trans} maps. (**d**) K_{ep} maps. (**e**) V_e maps. (**f-h**) Histograms of K^{trans} maps, K_{ep} maps and V_e maps, respectively. ROI, Region of interest

Statistical analysis

All data analyses were performed by SPSS (v26.0; Chicago, IL) and Medcalc(v19.6; Ostend, Belgium). Two-sided $p<0.05$ was considered statistically significant. Normally distributed variables are expressed as the means±standard deviations; abnormally distributed variables are expressed as the median with the first and third interquartile range. Respectively, the Kolmogorov-Smirnov test and the F-test were used to evaluate the normality and homogeneity of the variance of continuous variable. The independent t-test or Mann-Whitney U-test was used to compare quantitative parameters with histogram and texture features between two groups categorized based on molecular subtype (TNBC vs. non-TNBC) and AR status (AR+TNBC vs. AR-TNBC). The receiver operating characteristic curves (ROC) analysis was performed to evaluate the diagnostic performance of parameters between TNBC and non-TNBC and between AR+and AR-TNBC. Multivariate binary logistic regression (method: forward stepwise) was performed on the parameters that were significantly different between the TNBC and non-TNBC groups, and another ROC curve was drawn to determine the predictive accuracy of the model based on these parameters and to identify the best cut-off value for distinguishing TNBC.

Results

Patient clinicopathologic characteristics

In total, 99 patients with proven invasive ductal carcinoma were included in this study. The mean age of all the patients was 52.85±10.15 years (age range: 30–78 years). Of the 99 patients, 36 patients (36.3%) were histologically confirmed TNBC and 63 patients (63.6%) were non-TNBC. No significant difference between the TNBC and non-TNBC groups were found in age, axillary lymph node status, and ductal carcinoma in situ (DCIS) status ($p=0.959$, 0.243, 0.050, respectively). The features with statistically significant differences between the two groups were clinical T stage, histological grade, AR expression ($p=0.002$, < 0.001, < 0.001, respectively). There are no significant differences in clinicopathologic characteristics between AR+and AR-TNBC groups. The tables of patient's clinical pathologic characteristics were presented in Tables 1 and 2.

TNBC versus non-TNBC

After inter-observer agreement analysis, 261 histogram and texture features extracted from DCE-MRI were used for analysis. After the independent t-test and Mann-Whitney U-test, 9 parameters were found to be statistically different between the TNBC and non-TNBC groups, which were summarized in Table 3. The values

Table 1 Clinical and histopathologic characteristics of all people

Characteristics	non-TNBC (n = 63)	TNBC (n = 36)	p Value
Age	53.27 ± 10.49	52.11 ± 9.62	0.959
Histological grade			<0.001*
Low grade(grade 1 or 2)	52 (82.5%)	12 (33.3%)	
High grade(grade 3)	11 (17.5%)	24 (66.7%)	
Clinical T stage			0.002*
T1	45 (71.4%)	14 (38.9%)	
T2	18 (28.6%)	22 (61.1%)	
Axillary lymph node			0.243
Negative	42 (66.7%)	28 (77.8%)	
Positive	21 (33.3%)	8 (22.2%)	
DCIS status			0.050
Negative	46 (73.0%)	33 (91.7%)	
Positive	17 (27.0%)	3 (8.3%)	
AR			<0.001*
Negative	4 (6.3%)	20 (55.6%)	
Positive	59 (93.7%)	16 (44.4%)	

TNBC, Triple-negative breast cancer; non-TNBC, non-Triple-negative breast cancer; DCIS, Ductal carcinoma in situ; AR, Androgen receptor

* indicates statistical significance at $p < 0.05$

Table 2 Clinical and histopathologic characteristics of people with triple-negative breast cancer

Characteristics	AR-TNBC (n = 20)	AR + TNBC (n = 16)	p Value
Age	49.5 ± 10.31	55.38 ± 7.78	0.068
Histological grade			0.729
Low grade (grade 1 or 2)	6 (30.0%)	6 (37.5%)	
High grade (grade 3)	14 (70.0%)	10 (62.5%)	
Clinical T stage			0.500
T1	7 (35.0%)	8 (50.0%)	
T2	13 (65.0%)	8 (50.0%)	
Axillary lymph node			0.422
negative	17 (85.0%)	11 (68.8%)	
Positive	3 (15.0%)	5 (31.2%)	
DCIS status			0.574
Negative	19 (95.0%)	14 (87.5%)	
Positive	1 (5.0%)	2 (12.5%)	

AR-TNBC, Androgen receptor-negative triple-negative breast cancer; AR + TNBC, Androgen receptor-positive triple-negative breast cancer; DCIS, Ductal carcinoma in situ

Table 3 Parameters that significantly different in TNBC from non-TNBC

Parameter	non-TNBC(n = 63)	TNBC(n = 36)	p Value
K_{ep_Max}	3.075 ± 0.214	4.009 ± 0.316	0.018
$K_{ep\_MaxIntensity}$	2.809 (1.454, 3.621)	3.720 (2.545, 4.562)	0.014
K_{ep_Range}	2.804 (1.454, 3.580)	3.719 (2.545, 4.562)	0.014
$K_{ep\_Skewness}$	1.051 ± 0.083	1.407 ± 0.098	0.009
$V_{e\_Variance}$	0.061 ± 0.005	0.084 ± 0.006	0.003
$V_{e\_HaraVariance}$	0.059 ± 0.005	0.083 ± 0.006	0.002
$V_{e\_SumVariance}$	0.043 ± 0.003	0.062 ± 0.005	0.001
$V_{e\_StdDeviation}$	0.236 (0.167, 0.283)	0.279 (0.236, 0.338)	0.003
$V_{e\_ClusterProminence}(\times 10^7)$	3.594 (3.257, 9.856)	5.609 (4.687, 13.785)	0.004

The data in the table is represented by means ± standard deviations (normal distribution) or median (first and third quartiles) (skewed distribution). TNBC, Triple-negative breast cancer; non-TNBC, non-Triple-negative breast cancer

Table 4 Diagnostic value of histogram and texture parameters that can clearly distinguish TNBC from non-TNBC

Parameter	AUC	Standard Error	p Value	95% Confidence Interval	
				Lower Bound	Upper Bound
K_{ep_Max}	0.643	0.057	0.018	0.531	0.755
$K_{ep\_MaxIntensity}$	0.649	0.056	0.014	0.539	0.760
K_{ep_Range}	0.649	0.056	0.014	0.539	0.760
$K_{ep\_Skewness}$	0.664	0.055	0.007	0.555	0.773
$V_{e\_Variance}$	0.679	0.057	0.003	0.567	0.791
$V_{e\_HaraVariance}$	0.683	0.057	0.002	0.572	0.795
$V_{e\_SumVariance}$	0.701	0.056	0.001	0.592	0.811
$V_{e\_StdDeviation}$	0.679	0.057	0.003	0.567	0.791
$V_{e\_ClusterProminence}$	0.674	0.057	0.004	0.562	0.786

AUC, The area under the receiver operating characteristic curve

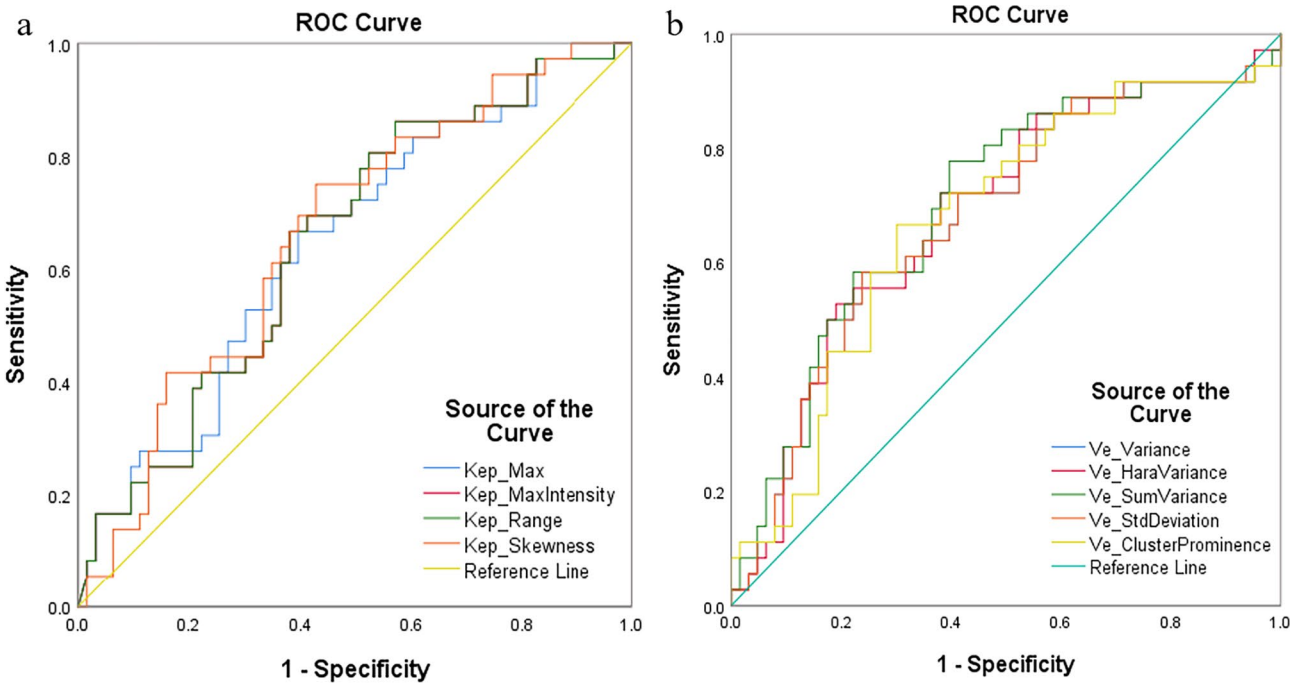

Fig. 2 ROC curves for (**a**) K_{ep}-related and (**b**) V_e-related parameters that significantly differed between TNBC and non-TNBC. ROC, Receiver operating characteristic; TNBC, Triple-negative breast cancer; non-TNBC, non-Triple-negative breast cancer

of these ten parameters were all significantly higher in TNBC than in non-TNBC. The ROC curves and the AUC for all parameters were summarized in Table 4; Fig. 2. $V_{e\_SumVariance}$ showed the largest area under the ROC curve (AUC=0.701, p=0001), and AUCs of other parameters were near 0.700.

In the multivariate logistic regression analysis, only K_{ep_Range} (odds ratio=1.326, p=0.032) and $V_{e\_SumVariance}$ (odds ratio=2.9×10^{10}, p=0.005) were associated with TNBC. The combined model was established based on these two parameters and the ROC curve was shown in Fig. 3. The AUC of the model for identifying TNBC was 0.735 (p<0.001), the cutoff value, sensitivity and specificity were 0.268, 88.89% and 52.38%, respectively.

AR+TNBC versus AR-TNBC

No histogram parameters were statistically different between the AR-TNBC and AR+TNBC groups. For the texture features, the values of $K_{ep\_Compactness2}$, $K_{ep\_SphericalDisproportion}$, and $V_{e\_GlcmEntropy}$ were significantly lower in the AR-TNBC group, which were summarized in Table 5. Table 6 showed the AUCs for these three parameters.

Discussion

Our study sought to assess tumor heterogeneity by pharmacokinetic parameters with histogram and texture characteristics in preoperative DCE-MRI images of breast cancer patients. The current study aimed to distinguish TNBC from non-TNBC and to identify whether AR is expressed in TNBC, which would provide important

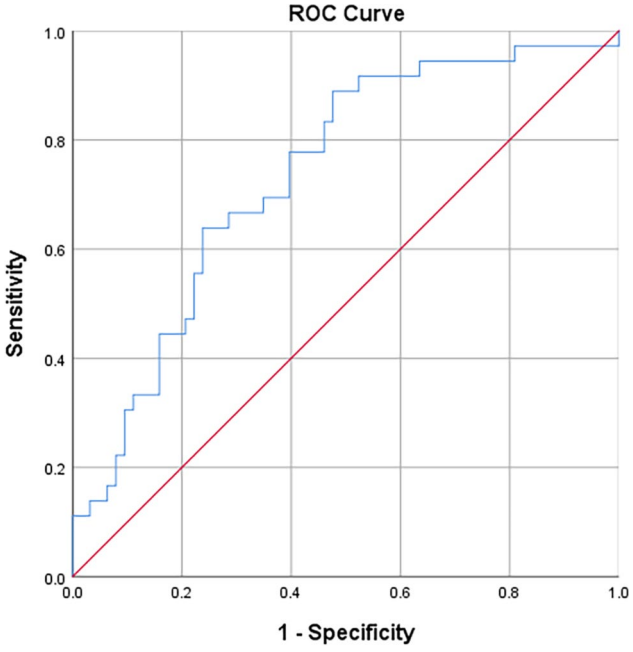

Fig. 3 ROC curve for the combined model (blue line). ROC, Receiver operating characteristic

imaging information for clinical treatment and prognosis prediction. We found that the K_{ep_Range} (p=0.032) and $V_{e\_SumVariance}$ (p=0.005) values of the TNBC group were higher than those of the non-TNBC group, and the AUC of their combined model was 0.735. The $K_{ep\_Compactness2}$, $K_{ep\_SphericalDisproportion}$, and $V_{e\_GlcmEntropy}$ values of the AR+TNBC group were higher than those of the AR-TNBC group, and their AUCs were all close to 0.700.

The incidence of TNBC in this study was approximately 36.3% of all breast cancers, which was higher than the 15–20% reported in previous study [3]. This may be attributed to the inclusion criteria of patients in this study and the differences in incidence rates in different regions. No difference in age and in the lymph node positivity rate was observed between TNBC and non-TNBC groups, although some studies have pointed out that TNBC is more likely to occur in younger women and has a higher lymph node positivity rate [4, 27]. The reason for this result may be that the number of patients was so small that the difference between the two groups did not reach statistical significance. Similar to previous reports [4, 28], TNBC in the present study was associated with higher histological grades.

Recently, several studies of TNBC MRI features have been reported. Morphologically, TNBC tends to present as a benign-like mass with a relatively circumscribed margin, which frequently shows internal high-signal intensity on T2-weighted images [29]. Under functional imaging, TNBC shows a higher apparent diffusion coefficient (ADC) on DWI because of a greater necrotic component [19]. On DCE-MRI, larger size, round/oval mass shape, smooth mass margin, rim and persistent enhancement pattern were useful features to detect TNBC [19, 30]. Through the quantitative analysis of DCE-MRI, several studies have observed significantly higher K_{ep} values in TNBC [31], which was similar to our results. Higher K_{ep} values are associated with increased vascular permeability, which may be attributed to the formation of new tumor vessels. However, the findings of Sung Hun Kim et al. were different and they believed that the K_{ep} value was independent of molecular subtype [32]. The reasons for this discrepancy may be related to differences in MRI protocols, study populations, ROI locations, and pharmacokinetic analysis software, and the substantial heterogeneity of breast cancers.

In our study, $K_{ep\_Skewness}$ represents the asymmetry of the probability distribution of the outflow rate of contrast agent between the interstitium and plasma. K_{ep_Range} represents the difference between the highest and lowest values of the outflow rate of contrast agent within VOI. The higher $K_{ep\_Skewness}$ and K_{ep_Range} of TNBC may be due to the fact that TNBC is densely packed with more aggressive components. Higher V_e values may imply poor tumor cellularity and an abundant tumor stroma, which includes fibroblasts, endothelial cells, and extracellular

Table 5 Parameters that significantly different in AR-TNBC from AR+TNBC

Parameter	AR-TNBC	AR+TNBC	p Value
$K_{ep\_Compactness2}$	15.120 (13.497, 16.024)	16.845 (15.118, 18.040)	0.049
$K_{ep\_SphericalDisproportion}$	1.261 (1.172, 1.314)	1.354 (1.264, 1.422)	0.049
$V_{e\_GlcmEntropy}$	7.300 (5.685, 9.015)	8.587 (8.312, 10.445)	0.008

AR-TNBC, Androgen receptor-negative triple-negative breast cancer; AR+TNBC, Androgen receptor-positive triple-negative breast cancer

Table 6 Diagnostic value of histogram and texture parameters that can clearly distinguish AR+TNBC from AR-TNBC

Parameter	AUC	Standard Error	p Value	95% Confidence Interval	
				Lower Bound	Upper Bound
$K_{ep\_Compactness2}$	0.694	0.097	0.018	0.504	0.883
$K_{ep\_SphericalDisproportion}$	0.694	0.097	0.014	0.504	0.883
$V_{e\_GlcmEntropy}$	0.756	0.089	0.014	0.581	0.931

AUC, The area under the receiver operating characteristic curve

matrix components that can provide growth factors and then stimulate angiogenesis [32]. Variance represents the mean of the squared distances of each value in the image ROI from the mean of the values and standard deviation (StdDeviation) measures the amount of variation or dispersion from the mean of the values in the image ROI. Skewness and StdDeviation are biomarkers of tumor heterogeneity [23], our study found higher $V_{e\_Variance}$ and $V_{e\_StdDeviation}$ values for TNBC, which was in part consistent with the findings of Ken Nagasaka et al. [33], reflecting the high heterogeneity of TNBC. Texture features such as $V_{e\_HaraVariance}$, $V_{e\_SumVariance}$ and $V_{e\_ClusterProminence}$ were different in TNBC and non-TNBC groups in our study, which were different from the texture features found in the previous studies [34, 35], we speculate the differences might be due to study populations, ROI locations and postprocessing softwares. Our study further validated that texture features and histogram analysis can distinguish TNBC from non-TNBC.

Several studies have suggested that AR could be a potential therapeutic target for TNBC [7, 11]. Although gene expression profiling is still the gold standard for molecular typing of breast cancer [6], it is not common as it is time consuming and expensive. Currently, IHC does not routinely express AR in some hospitals, so some studies have explored the use of imaging to identify AR+TNBC. Previous studies reported that the heterogeneously dense breast composition, masses with calcifications and irregular shape on mammography, masses with irregular shape or spiculated margins on sonography, mammographic calcifications with or without a mass, and non-mass enhancement on MRI were useful features to detect AR+TNBC [20, 36]. This was the first study to predict AR expression in TNBC using DCE-MRI-based pharmacokinetic parameters containing histograms and texture features, and the results of this study suggest that DCE-MRI-based pharmacokinetic parameters containing texture features can be used to identify AR expression in TNBC.

Compared with previous studies that evaluated the histogram features of DCE-MRI in the characterization of TNBC [33], we outlined the region of interest layer by layer around the edge of the tumor and finally obtained a VOI and enrolled both histogram and texture features of DCE-MRI. Hence, the conclusion derived from our study might provide more quantitative information within the whole tumor volume.

There are some notable limitations of our study. First, this is a single-center study and should be verified through multi-center studies with different imaging equipment and protocols. Second, the number of patients in this study was relatively small. Although this was a cohort study of 99 patients, including more patients in the subgroup analysis would make the results more reliable. Third, this study is a retrospective study and further verification is required in a prospective study. Fourth, the manual ROI segmentation is time-consuming, so more convenient and accurate ROI segmentation methods need to be further explored in the future.

Conclusions

The quantitative parameters of DCE-MRI and its corresponding histogram and texture parameters can help distinguish TNBC from non-TNBC and to identify whether AR is expressed in TNBC, which would provide important imaging information for clinical treatment and prognosis prediction.

Abbreviations

DCE-MRI	Dynamic contrast-enhanced magnetic resonance imaging
TNBC	Triple-negative breast cancer
non-TNBC	non-Triple-negative breast cancer
AR	Androgen receptor
AR+	AR-positive
AR-	AR-negative
ROC	Receiver operating characteristic
AUC	The area under the receiver operating characteristic curve
HER2	Human epidermal growth factor receptor 2
IHC	Immunohistochemistry
ER	Estrogen receptor
PR	Progesterone receptor
LAR	Luminal androgen receptor
DWI	Diffusion weighted imaging
TR	Repetition time
TE	Echo time
FOV	Field of view
TA	Total acquisition time
ROI	Region of interest
VOI	Volume of interest
EES	Extravascular extracellular space
ICC	Interclass correlation coefficient
FISH	Fluorescence in situ hybridization
DCIS	Ductal carcinoma in situ
ADC	Apparent diffusion coefficient

Acknowledgements

Not applicable.

Authors' contributions

Conception and design: WX, BZ; Administrative support: HL; The acquisition of data: WX, BZ; Collection and assembly of data: WX, BZ; Data analysis and interpretation: WX, JL, SL, HL; Writing the manuscript: All authors; All authors read and approved the final manuscript.

Funding

Not applicable.

Data Availability

The datasets used and/or analysed during the current study are available from the corresponding author on reasonable request.

Declarations

Competing interests

The authors declare no competing interests.

Ethics approval and consent to participate

The study was conducted in accordance with the Declaration of Helsinki (as revised in 2013). The Life Science Ethics Committee of Zhengzhou University approved this retrospective analysis and waived the need for informed consent.

Consent for publication
Not applicable.

Author details
[1]Department of Radiology, The Affiliated Cancer Hospital of Zhengzhou University & Henan Cancer Hospital, Zhengzhou 450008, China
[2]GE healthcare (China), Beijing 100176, China

Received: 11 April 2022 / Accepted: 23 May 2023
Published online: 01 June 2023

References

1. Sung H, Ferlay J, Siegel RL, Laversanne M, Soerjomataram I, Jemal A, Bray F. Global Cancer Statistics 2020: GLOBOCAN estimates of incidence and Mortality Worldwide for 36 cancers in 185 countries. CA Cancer J Clin. 2021;71(3):209–49.
2. Curigliano G, Burstein HJ, Winer EP, Gnant M, Dubsky P, Loibl S, Colleoni M, Regan MM, Piccart-Gebhart M, Senn HJ, et al. De-escalating and escalating treatments for early-stage breast cancer: the St. Gallen International Expert Consensus Conference on the primary therapy of early breast Cancer 2017. ANN ONCOL. 2017;28(8):1700–12.
3. Lin NU, Vanderplas A, Hughes ME, Theriault RL, Edge SB, Wong YN, Blayney DW, Niland JC, Winer EP, Weeks JC. Clinicopathologic features, patterns of recurrence, and survival among women with triple-negative breast cancer in the National Comprehensive Cancer Network. CANCER-AM CANCER SOC. 2012;118(22):5463–72.
4. Dent R, Trudeau M, Pritchard KI, Hanna WM, Kahn HK, Sawka CA, Lickley LA, Rawlinson E, Sun P, Narod SA. Triple-negative breast cancer: clinical features and patterns of recurrence. CLIN CANCER RES. 2007;13(15 Pt 1):4429–34.
5. Goldhirsch A, Winer EP, Coates AS, Gelber RD, Piccart-Gebhart M, Thurlimann B, Senn HJ. Personalizing the treatment of women with early breast cancer: highlights of the St Gallen International Expert Consensus on the primary therapy of early breast Cancer 2013. ANN ONCOL. 2013;24(9):2206–23.
6. Lehmann BD, Bauer JA, Chen X, Sanders ME, Chakravarthy AB, Shyr Y, Pietenpol JA. Identification of human triple-negative breast cancer subtypes and preclinical models for selection of targeted therapies. J CLIN INVEST. 2011;121(7):2750–67.
7. Gerratana L, Basile D, Buono G, De Placido S, Giuliano M, Minichillo S, Coinu A, Martorana F, De Santo I, Del ML, et al. Androgen receptor in triple negative breast cancer: a potential target for the targetless subtype. CANCER TREAT REV. 2018;68:102–10.
8. Hwang KT, Kim YA, Kim J, Park JH, Choi IS, Hwang KR, Chai YJ, Park JH. Influence of androgen receptor on the prognosis of breast Cancer. J CLIN MED 2020, 9(4).
9. Bozovic-Spasojevic I, Zardavas D, Brohee S, Ameye L, Fumagalli D, Ades F, de Azambuja E, Bareche Y, Piccart M, Paesmans M, et al. The prognostic role of androgen receptor in patients with early-stage breast Cancer: a Meta-analysis of clinical and gene expression data. CLIN CANCER RES. 2017;23(11):2702–12.
10. Di Leone A, Fragomeni SM, Scardina L, Ionta L, Mule A, Magno S, Terribile D, Masetti R, Franceschini G. Androgen receptor expression and outcome of neoadjuvant chemotherapy in triple-negative breast cancer. Eur Rev Med Pharmacol Sci. 2021;25(4):1910–5.
11. Jahan N, Jones C, Rahman RL. Androgen receptor expression in breast cancer: implications on prognosis and treatment, a brief review. MOL CELL ENDOCRINOL. 2021;531:111324.
12. Pietri E, Conteduca V, Andreis D, Massa I, Melegari E, Sarti S, Cecconetto L, Schirone A, Bravaccini S, Serra P, et al. Androgen receptor signaling pathways as a target for breast cancer treatment. Endocr Relat Cancer. 2016;23(10):R485–98.
13. Burge CN, Chang HR, Apple SK. Do the histologic features and results of breast cancer biomarker studies differ between core biopsy and surgical excision specimens? Breast. 2006;15(2):167–72.
14. Liu HL, Zong M, Wei H, Wang C, Lou JJ, Wang SQ, Zou QG, Jiang YN. Added value of histogram analysis of apparent diffusion coefficient maps for differentiating triple-negative breast cancer from other subtypes of breast cancer on standard MRI. CANCER MANAG RES. 2019;11:8239–47.
15. Tang WJ, Jin Z, Zhang YL, Liang YS, Cheng ZX, Chen LX, Liang YY, Wei XH, Kong QC, Guo Y, et al. Whole-lesion Histogram Analysis of the Apparent Diffusion Coefficient as a quantitative imaging biomarker for assessing the level of Tumor-Infiltrating lymphocytes: value in molecular subtypes of breast Cancer. FRONT ONCOL. 2020;10:611571.
16. Kim JJ, Kim JY, Suh HB, Hwangbo L, Lee NK, Kim S, Lee JW, Choo KS, Nam KJ, Kang T, et al. Characterization of breast cancer subtypes based on quantitative assessment of intratumoral heterogeneity using dynamic contrast-enhanced and diffusion-weighted magnetic resonance imaging. EUR RADIOL. 2022;32(2):822–33.
17. Wang H, Hu Y, Li H, Xie Y, Wang X, Wan W. Preliminary study on identification of estrogen receptor-positive breast cancer subtypes based on dynamic contrast-enhanced magnetic resonance imaging (DCE-MRI) texture analysis. Gland Surg. 2020;9(3):622–8.
18. Tsai WC, Chang KM, Kao KJ. Dynamic contrast enhanced MRI and Intravoxel Incoherent Motion to identify molecular subtypes of breast Cancer with different vascular normalization gene expression. KOREAN J RADIOL. 2021;22(7):1021–33.
19. Yetkin DI, Akpinar MG, Durhan G, Demirkazik FB. Comparison of clinical and magnetic resonance imaging findings of triple-negative breast cancer with non-triple-negative tumours. Pol J Radiol. 2021;86:e269–76.
20. Candelaria RP, Adrada BE, Wei W, Thompson AM, Santiago L, Lane DL. Imaging features of triple-negative breast cancers according to androgen receptor status. Eur J Radiol. 2019;114:167–74.
21. Gigli S, Amabile MI, David E, De Luca A, Grippo C, Manganaro L, Monti M, Ballesio L. Morphological and semiquantitative kinetic analysis on dynamic contrast enhanced MRI in Triple negative breast Cancer patients. ACAD RADIOL. 2019;26(5):620–5.
22. Li Z, Ai T, Hu Y, Yan X, Nickel MD, Xu X, Xia L. Application of whole-lesion histogram analysis of pharmacokinetic parameters in dynamic contrast-enhanced MRI of breast lesions with the CAIPIRINHA-Dixon-TWIST-VIBE technique. J MAGN RESON IMAGING. 2018;47(1):91–6.
23. Just N. Improving tumour heterogeneity MRI assessment with histograms. Br J Cancer. 2014;111(12):2205–13.
24. Jia ZZ, Geng DY, Liu Y, Chen XR, Zhang J. Microvascular permeability of brain astrocytoma with contrast-enhanced magnetic resonance imaging: correlation analysis with histopathologic grade. Chin Med J (Engl). 2013;126(10):1953–6.
25. Varghese BA, Cen SY, Hwang DH, Duddalwar VA. Texture analysis of imaging: what radiologists need to know. AJR Am J Roentgenol. 2019;212(3):520–8.
26. Sun K, Zhu H, Chai W, Zhan Y, Nickel D, Grimm R, Fu C, Yan F. Whole-lesion histogram and texture analyses of breast lesions on inline quantitative DCE mapping with CAIPIRINHA-Dixon-TWIST-VIBE. EUR RADIOL. 2020;30(1):57–65.
27. Whitman GJ, Albarracin CT, Gonzalez-Angulo AM. Triple-negative breast cancer: what the radiologist needs to know. SEMIN ROENTGENOL. 2011;46(1):26–39.
28. Anders C, Carey LA. Understanding and treating triple-negative breast cancer. Oncol (Williston Park). 2008;22(11):1233–9.
29. Huang Z, Tu X, Lin Q, Zhan Z, Tang L, Liu J, Lin D, Luo S, Zhang D, Ruan C. Intramammary edema of invasive breast cancers on MRI T2-weighted fat suppression sequence: correlation with molecular subtypes and clinical-pathologic prognostic factors. Clin Imaging. 2022;83:87–92.
30. Choi Y, Kim SH, Youn IK, Kang BJ, Park WC, Lee A. Rim sign and histogram analysis of apparent diffusion coefficient values on diffusion-weighted MRI in triple-negative breast cancer: comparison with ER-positive subtype. PLoS ONE. 2017;12(5):e177903.
31. Yang Z, Chen X, Zhang T, Cheng F, Liao Y, Chen X, Dai Z, Fan W. Quantitative multiparametric MRI as an imaging biomarker for the prediction of breast Cancer receptor status and molecular subtypes. FRONT ONCOL. 2021;11:628824.
32. Kim SH, Lee HS, Kang BJ, Song BJ, Kim HB, Lee H, Jin MS, Lee A. Dynamic contrast-enhanced MRI perfusion parameters as imaging biomarkers of Angiogenesis. PLoS ONE. 2016;11(12):e168632.
33. Nagasaka K, Satake H, Ishigaki S, Kawai H, Naganawa S. Histogram analysis of quantitative pharmacokinetic parameters on DCE-MRI: correlations with prognostic factors and molecular subtypes in breast cancer. BREAST CANCER-TOKYO. 2019;26(1):113–24.
34. Chang RF, Chen HH, Chang YC, Huang CS, Chen JH, Lo CM. Quantification of breast tumor heterogeneity for ER status, HER2 status, and TN molecular subtype evaluation on DCE-MRI. MAGN RESON IMAGING. 2016;34(6):809–19.
35. Fan M, Li H, Wang S, Zheng B, Zhang J, Li L. Radiomic analysis reveals DCE-MRI features for prediction of molecular subtypes of breast cancer. PLoS ONE. 2017;12(2):e171683.

36. Candelaria RP, Adrada BE, Wei W, Thompson AM, Santiago L, Lane DL, Huang ML, Arribas EM, Rauch GM, Symmans WF, et al. Imaging features of triple-negative breast cancers according to androgen receptor status. EUR J RADIOL. 2019;114:167–74.

Publisher's Note